Biochimica et Biophysica Acta 1833 (2013) 90–100

Contents lists available at SciVerse ScienceDirect

Biochimica et Biophysica Acta

journal homepage: www.elsevier.com/locate/bbamcr

Inhibition of ERK activation enhances the repair of double-stranded breaks via non-homologous end joining by increasing DNA-PKcs activation

Fengxiang Wei [a,b,c,d,e,*], Judy Yan [b,c,d,e], Damu Tang [b,c,d,e,**], Xiaozeng Lin [b,c,d,e,f], Lizhi He [b,c,d,e], Yanyun Xie [b,c,d,e,f], Lijian Tao [f], Shaojuan Wang [a]

[a] The Genetics Laboratory, Maternity and Child Healthcare Hospital, Longgang District, Shenzhen, Guangdong, PR China
[b] Division of Nephrology, Department of Medicine, McMaster University, Canada
[c] Division of Urology, Department of Surgery, McMaster University, Canada
[d] Father Sean O'Sullivan Research Institute, St. Joseph's Hospital, Hamilton, Ontario, Canada
[e] The Hamilton Center for Kidney Research, St. Joseph's Hospital, Hamilton, Ontario, Canada
[f] Division of Nephrology, Department of Medicine, Xiangya Hospital, Central South University, Changsha, Hunan, PR China

ARTICLE INFO

Article history:
Received 14 April 2012
Received in revised form 2 October 2012
Accepted 15 October 2012
Available online 23 October 2012

Keywords:
ERK1/2 kinases
DNA damage repair
Non-homologous end joining (NHEJ)
DNA damage response (DDR)
Ku
DNA-PKcs

ABSTRACT

Non-homologous end joining (NHEJ) is one of the major pathways that repairs double-stranded DNA breaks (DSBs). Activation of DNA-PK is required for NHEJ. However, the mechanism leading to DNA-PKcs activation remains incompletely understood. We provide evidence here that the MEK–ERK pathway plays a role in DNA-PKcs-mediated NHEJ. In comparison to the vehicle control (DMSO), etoposide (ETOP)-induced DSBs in MCF7 cells were more rapidly repaired in the presence of U0126, a specific MEK inhibitor, based on the reduction of γH2AX and tail moments. Additionally, U0126 increased reactivation of luciferase activity, which resulted from the repair of restriction enzyme-cleaved DSBs. Furthermore, while inhibition of ERK activation using the dominant-negative MEK1K97M accelerated the repair of DSBs, enforcing ERK activation with the constitutively active MEK1Q56P reduced DSB repair. In line with MEK activating ERK1 and ERK2 kinases, knockdown of either ERK1 or ERK2 increased DSB repair. Consistent with the activation of DNA-PKcs being required for NHEJ, we demonstrated that inhibition of ERK activation using U0126, MEK1K97M, and knockdown of ERK1 or ERK2 enhanced ETOP-induced activation of DNA-PKcs. Conversely, enforcing ERK activation by MEK1Q56P reduced ETOP-initiated DNA-PKcs activation. Taken together, we demonstrate that ERK reduces NHEJ-mediated repair of DSBs via attenuation of DNA-PKcs activation.

1. Introduction

Double-stranded DNA breaks (DSBs) are the most toxic form of DNA lesions. DSBs can be generated endogenously during cellular processes including immunoglobin gene rearrangement [V(D)J recombination] and meiotic recombination as well as exogenously by DNA damage reagents such as ionizing radiation (IR) and etoposide, a topoisomerase poison [1,2]. Compromising the process of DSB repair could result in radiation-sensitive and severe combined immune deficiency (SCID) in humans (RS-SCID) [3,4] and in mice [5,6].

DSBs are repaired by two major pathways, homologous recombination (HR) and non-homologous end joining (NHEJ) [2]. NHEJ, which is not restricted to specific phases of the cell cycle, is the major pathway that repairs IR-induced DSBs and the DSBs that are not associated with replication [1,2]. The core machinery of NHEJ consists of DNA-PK (the DNA-dependent protein kinase), end processing factors, and the XRCC4/DNA ligase IV complex [7,2]. The DNA-PK complex forms when the catalytic subunit (DNA-PKcs) binds to DSBs and the Ku (Ku70/80 heterodimer) proteins [2]. The first event of a NHEJ reaction is Ku-mediated recognition of DSBs, which leads to the association of DNA-PKcs with both Ku and double-stranded (ds) DNA ends, resulting in substantial increases in the protein kinase activity of DNA-PKcs [7,2].

While it is well documented that activation of DNA-PKcs is essential in the initiation of the NHEJ process [8,2], mechanisms governing DNA-PKcs activation is less understood. DNA-PKcs belongs to the family of PI3 kinase related kinases (PIKKs), which include ATM, ATR, and DNA-PKcs. PIKKs possess typical structural features, including a FAT, a kinase, and a C-terminal FATC domain [9]. These features underlie as to why activation of PIKKs involves binding to specific proteins and interaction with DNA lesions [10]. DNA-PKcs activation is primarily mediated by binding to Ku in the presence of dsDNA ends [11,12]. In vitro interaction with DNA-bound Ku is sufficient to activate DNA-PKcs [11,13]. Activation of DNA-PKcs results in autophosphorylation at residues within two major clusters, the ABCDE

* Correspondence to: F. Wei, The Genetics Laboratory, Maternity and Child Healthcare Hospital, 50 Aixin road, Shenzhen, Guangdong, PR China 518100. Tel.: +86 13088883678.
** Correspondence to: D. Tang, T3310, St. Joseph's Hospital, 50 Charlton Ave East, Hamilton, Ontario, Canada, L8N 4A6. Tel.: +1 905 522 1155x35168; fax: +1 905 521 6181.
E-mail addresses: haowei727499@163.com (F. Wei), damut@mcmaster.ca (D. Tang).

0167-4889/$ – see front matter. Crown Copyright © 2012 Published by Elsevier B.V. All rights reserved.
http://dx.doi.org/10.1016/j.bbamcr.2012.10.016

and PQR cluster [14,8,15], as well as at threonine (T) 3905 in the T-loop located in the kinase domain [16]. These autophosphorylation events cause conformational changes in DNA-PK, which mediates the subsequent steps in DSB repair [17].

While in vitro Ku and dsDNA ends are sufficient to activate DNA-PKcs, it is most likely that activation of DNA-PKcs in vivo requires additional factors. However, the identities of these factors remain largely unknown. We and others have recently demonstrated that the MEK–ERK pathway plays a role in DDR. ERK1 and ERK2 are members of the mitogen-activated protein kinase (MAPK) family [18] and are activated by the upstream kinases, MEK1 and MEK2 [19]. Activation of ERK kinases was observed in DDR that was induced by multiple DNA damage reagents [20–24]. While ERK activity facilitates DNA damage-induced cell cycle arrest or apoptosis in several mammalian cell lines and *Drosophila* [22,23,25–28], ERK activation also prevents DNA damage-induced apoptosis [24,29,30]. ERK mediates these DDR events downstream of either ATM [31] or ATR [26]. Experimental evidence also exists to place ERK upstream of ATM and ATR activation during DDR. It has been reported that the MEK–ERK pathway facilitates DNA damage-induced activation of ATM and ATR [31,32,25,33]. However, whether ERK plays a role in DNA-PK dependent NHEJ remains unclear.

We report here that inhibition of ERK activation via a variety of means enhances the repair of etoposide-induced DSBs by the sensitization of DNA-PKcs activation. Conversely, enforcing ERK activation using the constitutively active MEK1Q56P reduces NHEJ-mediated repair of DNA lesions which is associated with attenuation of DNA-PKcs activation. Taken together, we demonstrate here that ERK kinases attenuate DSB repair by reducing DNA-PKcs activation.

2. Material and methods

2.1. Materials and cell lines

Etoposide and Neocarzinostatin (NCS) were purchased from Sigma. MEK1 inhibitor U0126 was obtained from Sigma and dissolved in DMSO. MCF7 cells were purchased from ATCC and cultured in DMEM, supplemented with 10% FBS. The pGL2-control vector was purchased from Promega.

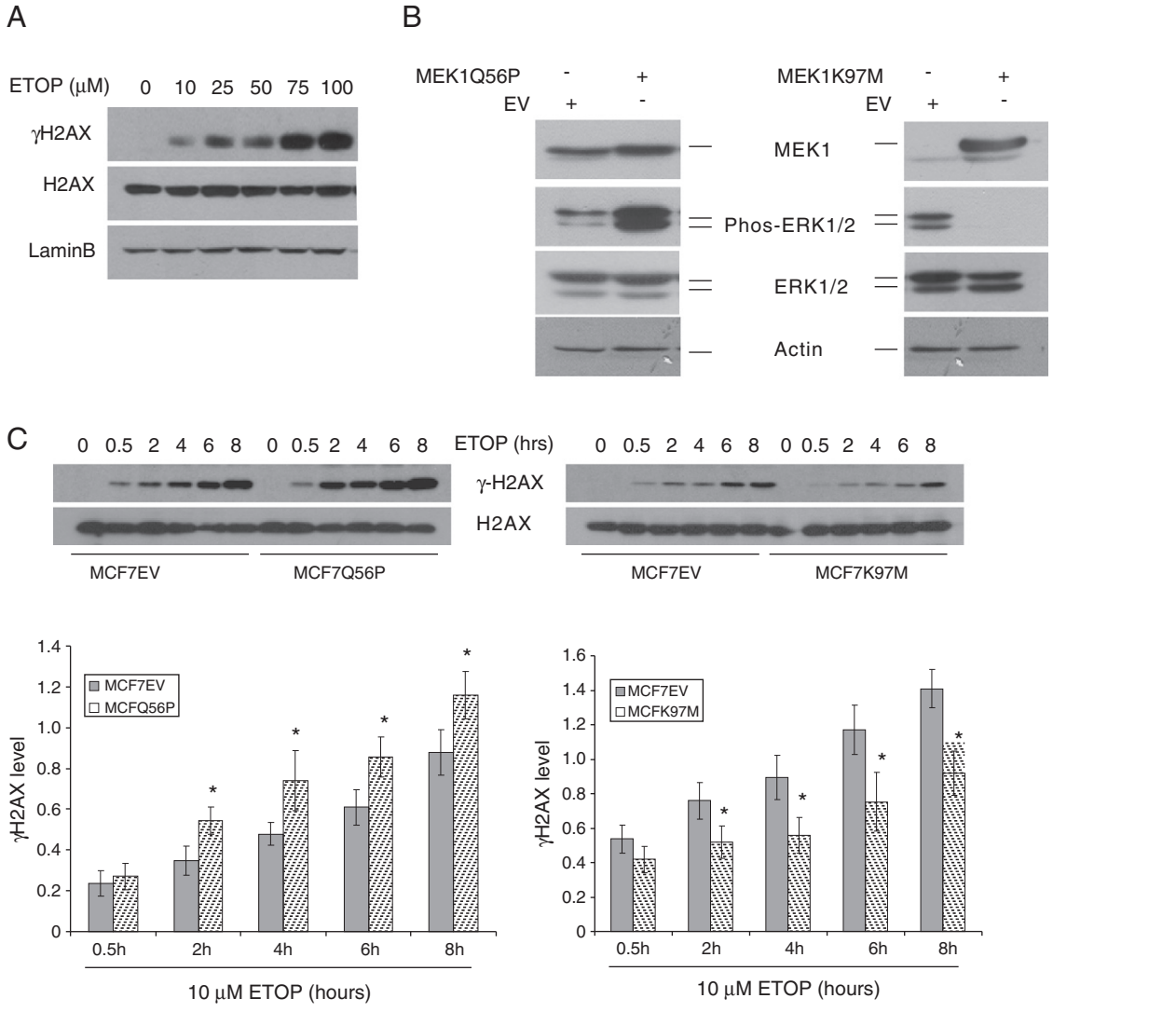

Fig. 1. ERK activity enhances the accumulation of γH2AX in MCF7 cells. (A) MCF7 cells were treated with the indicated doses of ETOP for 8 h and then examined for the expression of γH2AX, H2AX, and Lamin B by western blot. (B) MCF7 cells were stably expressed with an empty vector (EV), the constitutively active MEK1Q56P, or the dominant-negative MEK1K97M. Their expected impact on ERK activation was confirmed by western blot. (C) MCF7 EV, MEK1Q56P, and MEK1K97M cells were treated with DMSO (0) or 10 μM ETOP for the indicated period of time, followed by examination of γH2AX and H2AX by western blot. Experiments were repeated three times and representative images of a single experiment were shown (top panels). Quantification of three independent experiments (bottom panels). Means and standard errors (SE) were presented. *: statistically significant ($p<0.05$) in comparison to the respective DMSO treatments.

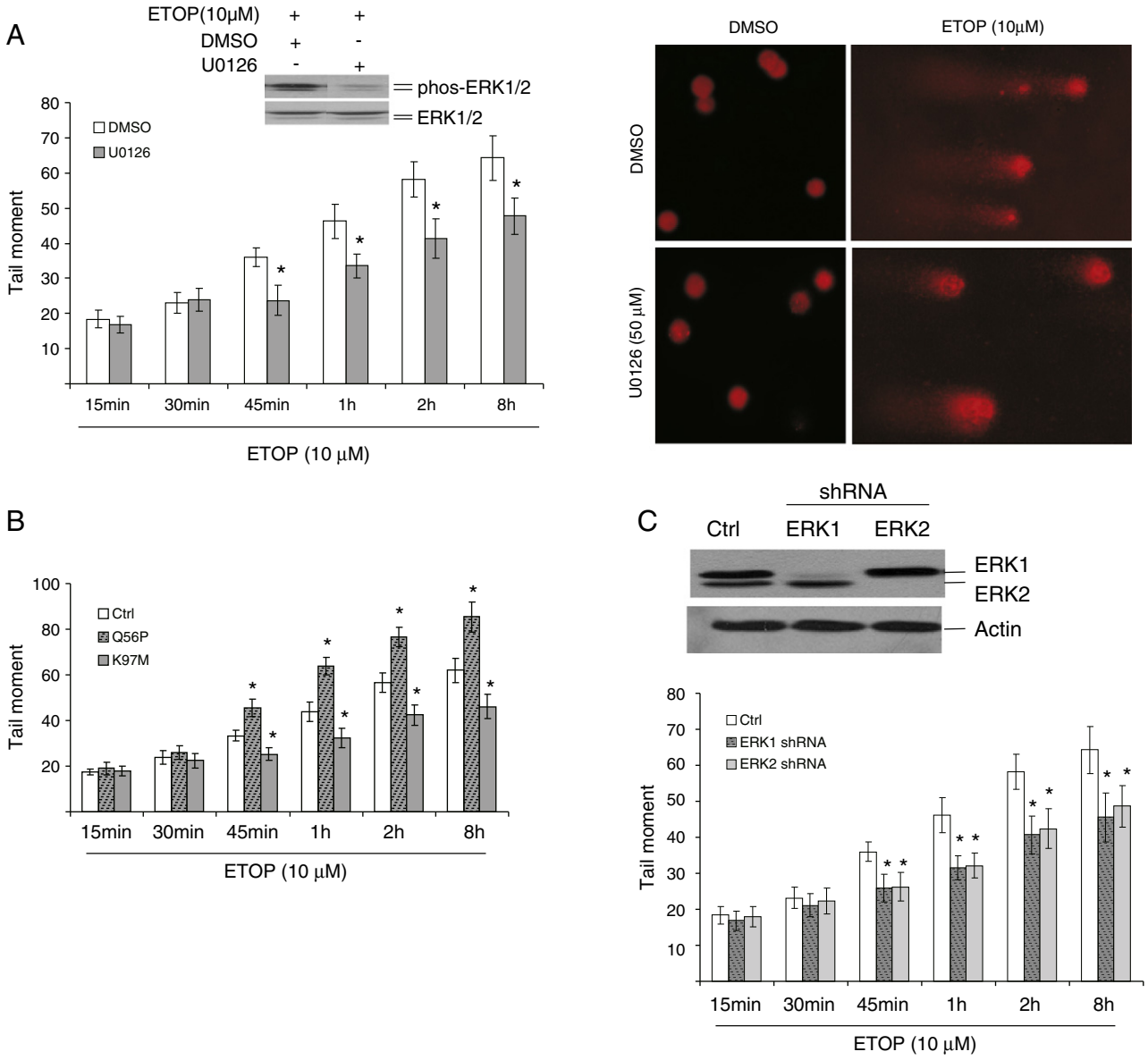

Fig. 2. Inhibition of ERK activation reduced DNA lesions upon prolonged ETOP treatment. (A) MCF7 cells were pre-treated with DMSO or U0126 (50 μM) for 30 min before addition of 10 μM ETOP for the indicated period of time, followed by comet assay. ERK inhibition by U0126 was determined by western blot (inset). Experiments were repeated three times and representative images of a single experiment at 8 h were shown (right panel). At least 100 nuclei were analyzed for tail moments. Means and standard errors (SE) were presented (left panel). *: statistically significant ($p<0.05$) in comparison to the respective DMSO treatments. (B) The indicated cell lines were treated with 10 μM ETOP, followed by examination for DNA breaks by comet assay and analyzed as described above. Experiments were repeated three times. *: statistically significant ($p<0.05$) in comparison to EV cells. (C) ERK1 or ERK2 in MCF7 cells was stably knocked-down using specific shRNA (top panel) and the kinetics of ETOP-induced DSBs was then examined by comet assay and analyzed. Experiments were repeated three times. *: statistically significant ($p<0.05$) in comparison to Ctrl cells.

2.2. Knockdown of ERK1 and ERK2 in MCF7 cells

Hairpin-based ERK1 and ERK2 shRNA plasmids (pSUPER-Erk1shRNA, pSUPER-Erk2shRNA) were reported to knockdown ERK1 and ERK2 in multiple myeloma cells [34]. These constructs were kindly provided by Dr. Chatterjee. We co-transfected MCF7 cells with pSUPER, pSUPER-Erk1shRNA, or pSUPER-Erk2shRNA, which do not possess an antibiotic selection marker, together with pcDNA3 (containing a Geneticin or G418 selection marker) at a ratio of 1:10 (pcDNA3: pSUPER, pSUPER-Erk1shRNA, or pSUPER-Erk2 shRNA). Cells were cultured in DMEM supplemented with G418 (1.5 mg/ml) for 3–4 weeks. Surviving cell colonies were examined for the knockdown of ERK1 and ERK 2 by western blot. Cells transfected with pSUPER + pcDNA3 were named as MCF7 Ctrl (control) cells.

2.3. Cell lysis and western blot

Cell lysates were prepared in a buffer containing 20 mM Tris (pH 7.4), 150 mM NaCl, 1 mM EDTA, 1 mM EGTA, 1% Triton X-100, 25 mM sodium pyrophosphate, 1 mM NaF, 1 mM β-glycerophosphate, 0.1 mM sodium orthovanadate, 1 mM PMSF, 2 μg/ml leupeptin and 10 μg/ml aprotinin. Total cell lysate containing 50 μg protein was separated on SDS-PAGE gel and transferred onto Immobilon-P membranes (Millipore). Membranes were blocked with 5% skim milk, followed by incubation with the indicated antibodies overnight at 4 °C. Signals were detected using an ECL Western Blotting Kit (Amersham). Primary antibodies and concentrations used are indicated as follows: anti-DNA-PKcs (1:1000; Abcam), anti-phospho-S2056 DNA-PKcs (1:1000; Abcam), anti-H2AX (1:1000; Cell Signalling), anti-γH2AX

(1:1000; Upstate), anti-lamin B (1:1000; Santa Cruz), anti-Ku70 (1:1000; Abcam), and anti-Ku80 (1:10,000; Abcam).

2.4. Immunofluorescence staining

Immunofluorescence staining was carried out by fixing cells with 4% paraformaldehyde for 15 min. The primary antibodies, anti-γH2AX (Upstate; 0.5 μg/ml), anti-phospho-S2056 DNA-PKcs (1:100; Abcam), and anti-Ku70 (1:100; Abcam), were added to the slides at 4 °C overnight, which was followed by incubation with the indicated secondary antibodies [Rhodamine-Donkey anti-rabbit IgG (1:200, Jackson Immuno Research Lab)] for 1 h at room temperature. The slides were subsequently covered with the VECTASHIELD mounting medium with DAPI (VECTOR Lab Inc., Burlingame, CA94010). Images were taken using a fluorescent microscope (Carl Zeiss, Axiovert 200) and processed by Photoshop and CorelDRAWx4.

2.5. Alkaline comet assay

Comet assay was performed following a published procedure [35]. Briefly, after specific treatments, cells were mixed with low melting point (LMP) agarose, applied to a 0.7% LMP agarose-coated slide, and lysed in a lysis buffer [2.5 M NaCl, 100 mM EDTA, 10 mM Tris (pH 10.0), 1% sodium lauroyl sarcosinate, 1% Triton X-100, and 10% DMSO] for 1 h at 40 °C in the dark. Unwinding of DNA was performed in running buffer (300 mM NaOH, 1 mM EDTA) for 40 min at 40 °C in dark, followed by electrophoresis in the same buffer at 25 V (0.7 V/cm) for 20 min at 40 °C in dark. Slides were neutralized in a buffer containing 0.4 M Tris–HCl (pH7.5) for 15 min with changes every 5 min. Slides were then stained with DAPI (2 μg/ml). Images were acquired with a fluorescent microscope (Carl Zeiss, Axiovert 200). At least 100 nuclei were analyzed for tail moment using the comet assay software project.

2.6. Ex vivo NHEJ assay

This assay was performed according to the published methodology [36]. In brief, pGL2-control (pGL2) construct was digested with either HindIII or EcoRI to completion, which was confirmed by DNA electrophoresis. Digested DNA was gel-purified. MCF7 cells were transiently transfected, using the TransIT-2020 Transfection reagent (Mirus Bio LLC), with undigested pGL2/β-Gal (2:1) or digested pGL2/β-Gal in triplicate for 48 h. Luciferase and β-Gal activity were determined using a commercial kit (Promega). Luciferase activity was first normalized against the respective β-Gal activity. Normalized luciferase activity derived from restriction enzyme-digested pGL2 was then expressed as the percentage of the normalized luciferase activity derived from uncut pGL2. Experiments were repeated three times. Means and standard errors were calculated using Excel.

2.7. Cell survival assay

The designated cells were seeded in duplicate at 2×10^4cells/well in 6-well plates for 24 h. Cells were then treated with DMSO (mock treatment) or ETOP at the designated doses for 8 h, followed by culturing in untreated medium for one week before the mock-treated cells became confluent. Surviving cells were then stained with crystal violet (0.5%). Three empty wells were also stained as background.

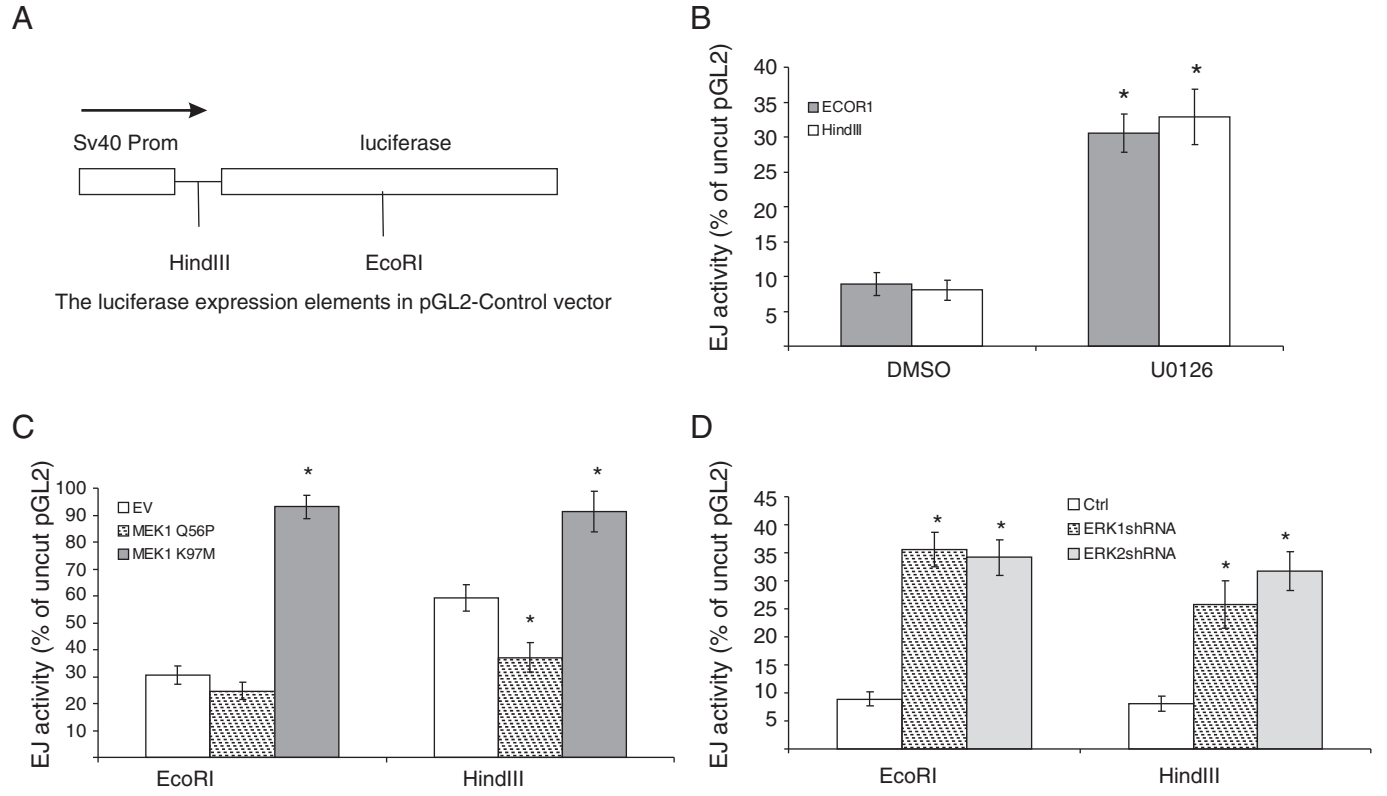

Fig. 3. Attenuation of ERK activation enhances NHEJ-mediated repair of DSBs. (A) Illustration of an ex vivo assay for cellular end-joining (EJ) activity. pGL2-control (pGL2) vector is cleaved by either HindIII or EcoRI, followed by transient transfection into MCF7 cells. Repair of restriction enzyme-generated double-stranded breaks reactivates luciferase activity. (B) MCF7 cells were pre-treated with DMSO or U0126 (50 μM) for 30 min, and then transfected with pGL2/β-Gal (at ratio of 2:1), HindIII-pGL2/β-Gal, or EcoRI-pGL2/β-Gal for 48 h, followed by determination of luciferase and β-Gal activities. Luciferase activity was first normalized against β-Gal activity. Normalized luciferase activity derived from HindIII-pGL2 or EcoRI-pGL2 was expressed as the percentage of the normalized luciferase activity derived from uncut pGL2. Experiments were carried out in triplicates and repeated three times. Means and standard errors are presented. *: statistically significant ($p<0.05$) in comparison to the respective DMSO treatments. (C, D) The indicated cell lines were examined for their EJ activity following the condition as described above. Experiments were carried out in triplicates and repeated three times. Means and standard errors are presented. *: statistically significant ($p<0.05$) in comparison to EV (C) or Ctrl (D) cells.

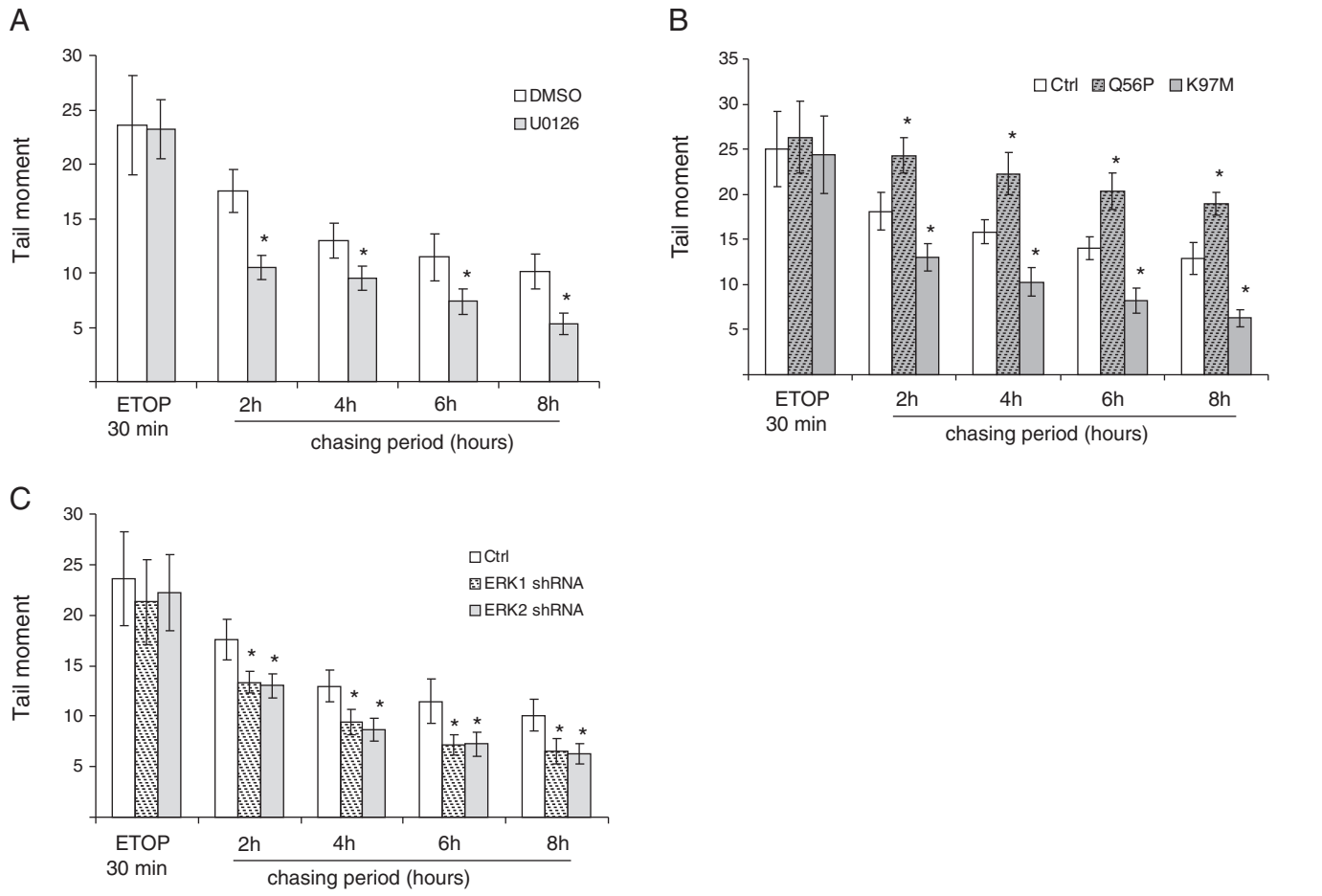

Fig. 4. Inhibition of ERK activation enhances the repair of ETOP-induced DSBs. (A) MCF7 cells were pre-treated for 30 min with DMSO or U0126 (50 μM) and then exposed for 30 min with 10 μM ETOP in the presence of DMSO or U0126 (50 μM). ETOP was then removed and cells were chased for the indicated period of time in fresh media containing either DMSO or U0126 (50 μM). DNA breaks were examined by comet assay. At least 100 nuclei were analyzed for tail moments. Experiments were repeated three times. Means and standard errors are presented. *: statistically significant ($p<0.05$) in comparison to the respective DMSO treatments. (B, C) The indicated cell lines were treated with 10 μM ETOP for 30 min, followed by chase treatment as indicated. DNA breaks were examined by comet assay and analyzed as stated above. Experiments were repeated three times. Means and standard errors are presented. *: statistically significant ($p<0.05$) in comparison to the respective Ctrl cells.

Staining was dissolved in 33% acetic acid and absorbance was read by a spectrometer at 550 nm. Specific staining was then derived by the subtraction of background staining.

2.8. Statistical analysis

Statistical analysis was performed using student *t*-test and $p<0.05$ was considered statistically significant.

3. Results

3.1. Attenuation of ERK activation reduces etoposide-induced DSBs in MCF7 cells

Etoposide (ETOP) stabilizes topoisomerase II-associated DNA breaks, and thereby preventing topoisomerase II-mediated ligation of cleaved DNA ends, resulting in the production of DSBs in the cell [37]. We have recently observed that knockdown of either ERK1 or ERK2 significantly reduces γH2AX in MCF7 cells during an 8-hour treatment with ETOP [32]. As γH2AX is a well regarded surrogate marker of DSBs, the above observations suggest that modulation of ERK activation affects the accumulation or repair of DSBs. To address this possibility, we have examined the kinetics of ETOP-induced γH2AX expression under different conditions of ERK activation. Evidenced by the induction of γH2AX, 10 μM ETOP induces DSBs (Fig. 1A). When the constitutively active MEK1Q56P was ectopically expressed in MCF7 cells, ERK activation was elevated (Fig. 1B) and 10 μM ETOP induced more γH2AX (Fig. 1C, Supplementary Fig. 1). Conversely, when ERK activation was reduced in MCF7 MEK1K97M cells in comparison to MCF7 EV cells (Fig. 1B), 10 μM ETOP induced less γH2AX ((Fig. 1C, Supplementary Fig. 1). However, we noticed that at the 0.5 h treatment with 10 μM ETOP, neither MEK1Q56P nor MEK1K97M MCF7 cells contained significantly different amounts of γH2AX than EV MCF7 cells (Fig. 1C). Collectively, these observations reveal that ERK activity facilitates the accumulation of γH2AX, indicative of the accumulation of DSBs.

To quantify DSB accumulation, we measured the tail moments using the comet assay under most widely used alkaline condition. Although the comet assay was believed to specifically detect single-stranded and double-stranded breaks under alkaline and neutral conditions, respectively, evidence presented in the recent International Comet Assay conference revealed that this was a misconception as the comet assay simply detects DNA breaks, both single-stranded and double-stranded breaks, performed at both alkaline and neutral conditions [38,39]. Consistent with this notion, alkaline comet assay is commonly used to detect DSBs [40–42]. In comparison with the vehicle control (DMSO), U0126 (the specific MEK inhibitor) does not affect ETOP-induced DSBs in the first 30 min of the treatment (Fig. 2A). However, U0126 reduces ETOP-induced DNA

breaks upon prolonged treatment (Fig. 2A, typical image shown on right panel). Similar results were also obtained when the dominant negative MEK1K97M was used. As expected, MEK1K97M inhibited the activation of ERK1 and ERK2 (Fig. 1B). In comparison to EV (empty vector) cells, MEK1K97M cells showed reduction of DNA breaks after treatment beyond 45 min (Fig. 2B). Conversely, enforced ERK activation by overexpression of the constitutively active MEK1Q56P in MCF7 cells (Fig. 1B) yielded comparable levels of DSBs in comparison with EV transfected cells at early phases of ETOP treatment, but elevated the DSB content at later time points (Fig. 2B). Collectively, the above observations suggest that attenuation of ERK activation enhances the accumulation of DSBs in MCF7 cells upon prolonged treatment with ETOP.

To further demonstrate the above concept, we recently established MCF7 cell lines in which either ERK1 or ERK2 was stably knocked-down using specific shRNAs (Fig. 2C, top panel) [32]. Knockdown of either ERK1 or ERK2 also does not affect ETOP-induced DSB accumulation in the early phases but reduces it at later time

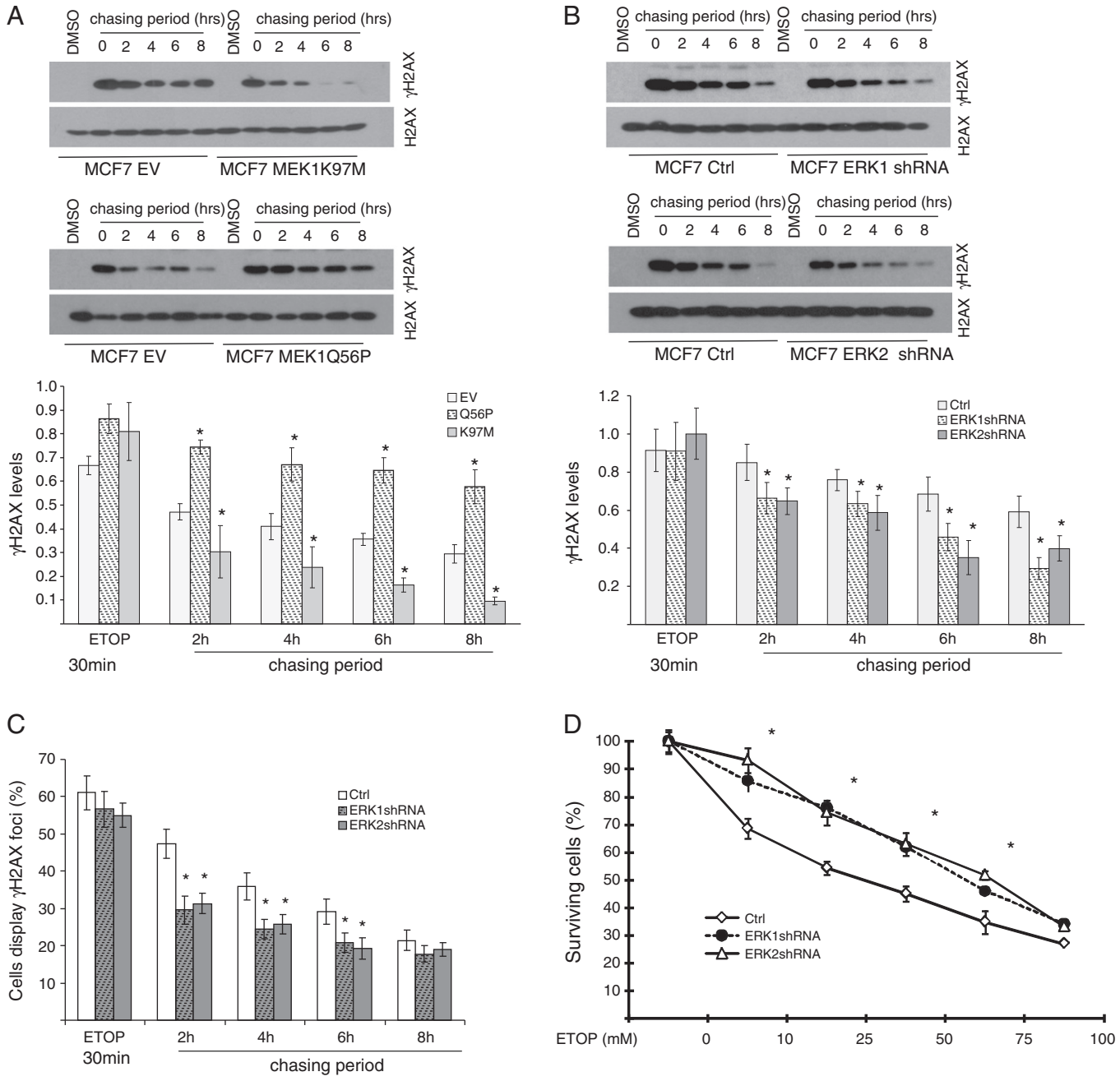

Fig. 5. ERK activation reduces the recovery from ETOP-induced DSBs. (A, B) The indicated cell lines were treated with 10 μM ETOP for 30 min and then chased for the indicated period of time. H2AX and γH2AX were examined by western blot. Levels of γH2AX were quantified against the respective H2AX. Experiments were repeated three times. A typical image is shown (A, B, top two panels). Means and standard errors are presented. *: statistically significant ($p<0.05$) in comparison to EV or Ctrl cells. (C) Ctrl, ERK1 shRNA, and ERK2 shRNA cells were treated with 10 μM ETOP for 30 min and then chased as indicated. Immunofluorescent staining was performed for γH2AX. The percentage of cells displaying γH2AX foci was determined by randomly counting 200 cells in several fields. Experiments were repeated three times. Means and standard errors are presented. *: statistically significant ($p<0.05$) in comparison to the respective Ctrl cells. (D) Ctrl, ERK1 shRNA, and ERK2 shRNA cells were seeded at 2×10^4 cells/well in 6-well plates one day prior to treatment with DMSO (0) or ETOP at the indicated doses for 8 h. Cells were then cultured in normal medium for one week. Surviving cells were stained with crystal violet, quantified, and expressed as percentage of the mock-treated cells. Experiments were repeated three times. Means and standard errors are presented. *: statistically significant ($p<0.05$) in comparison to the respective Ctrl cells.

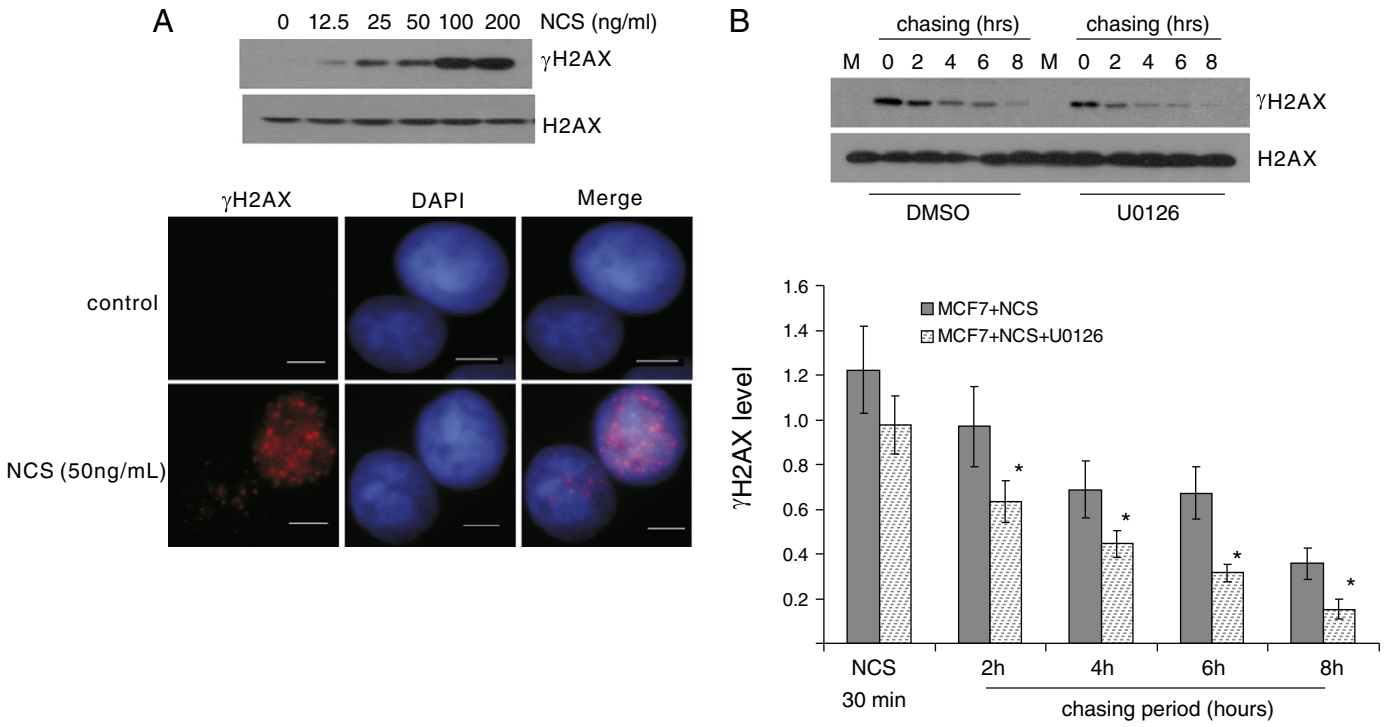

Fig. 6. Repair of NCS-induced DSBs is enhanced when ERK activation is reduced. (A) The kinetics of NCS-induced DSBs (γH2AX) in MCF7 cells (top panel). Experiments were repeated three times and representative images of a single experiment with 50 ng of NCS is shown (bottom panel). Scale bars represent 5 μm. (B) MCF7 cells were pre-treated for 30 min with DMSO or U0126 (50 μM), exposed for 30 min with NCS at 50 ng/ml, and then chased with or without (DMSO) or U0126 for the indicated periods of time. The levels of γH2AX and H2AX were determined by western blot. Experiments were repeated three times. Typical images from a single experiment were shown (top panel). Means and standard errors are presented (bottom panel). *: statistically significant ($p<0.05$) compared to samples without addition of U0126 (DMSO treated).

points (Fig. 2C, bottom panel, for typical image see Supplementary Fig. 2).

3.2. Inhibition of ERK activation enhances NHEJ-mediated end-joining activity

The above observations strongly suggest that ERK kinase activity negatively regulates the repair of ETOP-induced DSBs. To directly test this possibility, we measured NHEJ-mediated end-joining activity using an ex vivo assay (Fig. 3A) [36]. This type of ex vivo assay is widely used to assay cells' NHEJ capacity [36,43,44]. The assay detects the repair of a luciferase reporter construct (pGL2) that is cleaved by specific restriction enzymes (Fig. 3A). Repair of HindIII cleavage in the linker region between the SV40 promoter and the luciferase coding region enables luciferase expression even in the presence of mutations (Fig. 3A). Repair of EcoR1 cleavage within the lucifease coding region needs to be precise in order to produce functional luciferase (Fig. 3A). Therefore, this assay measures total (HindIII cleavage) and precise (EcoRI cleavage) end-joining activities (Fig. 3A) [36]. Since there is no intact homologous DNA strand available, this ex vivo assay largely measures the cellular NHEJ activity [36].

When using this assay to detect NHEJ-mediated end-joining activity, it was found that U0126 significantly increased both overall and precise end-joining activities in comparison to DMSO (Fig. 3B). While overexpression of the dominant negative MEK1K97M enhanced end-joining activity in comparison to EV cells, ectopic expression of the constitutively active MEK1Q56P reduced the end-joining activity (Fig. 3C). Furthermore, knockdown of either ERK1 or ERK2 also enhanced the repair of restriction enzyme cleaved DNA breaks (Fig. 3D). Taken together, we demonstrated that attenuation of ERK activation enhances cellular NHEJ activity. However, we could not distinguish the impact of ERK activation on the activity of overall end-joining versus that of precise end-joining. This might be attributable to the nature of this assay. As the breaks produced by HindIII and EcoRI are simple and competent for ligation, repair of these DSBs may not require the processing of dsDNA ends. Therefore, repair of these breaks may be much more precise than the repair of DSBs induced by DNA damage reagents. This possibility is supported by observations reported by others [36].

3.3. ERK activity reduces the repair of ETOP-induced DSBs

To examine whether attenuation of ERK activation facilitates the repair of ETOP-induced DSBs, MCF7 cells were treated with 10 μM ETOP for 30 min, which produces readily detectable tail moments examined by comet assay (Supplementary Fig. 3), followed by a period of chase (i.e. removal of ETOP) to allow DSB repair. In comparison with DMSO, 50 μM U0126, which potently inhibits ERK activation (Fig. 2A,inset), significantly enhanced the reduction of tail moments (Fig. 4A). Inhibition of ERK activation in cells expressing the dominant negative MEK1K97M also promoted the reduction of tail moments compared to EV cells (Fig. 4B). Conversely, the constitutively active MEK1Q56P, which activates ERK, slowed down the decrease in tail moments in comparison to EV (Fig. 4B). Consistent with these observations, knockdown of either ERK1 or ERK2 also promoted the repair of ETOP-induced DSBs, based on the observed reduction of tail moments in ERK1 shRNA and ERK shRNA cells in comparison to Ctrl cells (Fig. 4C).

To consolidate the above observations, we were able to show that while the dominant negative MEK1K97M accelerated the decreases of γH2AX during the periods of an 8 hour chase, the constitutively active MEK1Q56P significantly reduced this process in comparison to EV ((Fig. 5A, Supplementary Fig. 4). Furthermore, although a 30-minute treatment with 10 μM ETOP produced comparable levels of γH2AX in Ctrl, ERK1 shRNA, and ERK2 shRNA cells (Fig. 5B), γH2AX was reduced in an accelerated fashion in ERK1 shRNA and ERK2 shRNA cells

compared to Ctrl cells following the chase period (Fig. 5B). Additionally, the percentage of cells showing γH2AX foci was also reduced more rapidly in ERK1 shRNA and ERK2 shRNA cells than in Ctrl cells ((Fig. 5C, Supplementary Fig. 5). At the 8 hour chase, a number of cells displaying γH2AX foci were greatly reduced in all cell lines, which may be attributable to no significant differences being detected then among all cell lines (Fig. 5C).

To address whether enhancing DSB repair promotes cell survival following ETOP treatment, we treated Ctrl, ERK1 shRNA, and ERK2 shRNA cells with increasing doses of ETOP for 8 h and then examined the cell's survival capacity using a clonogenic assay. In comparison to the respective mock (DMSO) treatments, ERK1 shRNA and ERK2 shRNA cells survived better than Ctrl cells (Fig. 5D).

We subsequently demonstrated that ERK activity-mediated reduction of DSB repair is not limited to DSBs induced by ETOP. NCS (Neocarzinostatin) is a well-demonstrated radiomimetic drug. At 50 ng/ml, NCS clearly induced DSBs based on the appearance of γH2AX (Fig. 6A). While at the 30 minute time point, NCS induced comparable amount of γH2AX in MCF7 cells treated with either DMSO or U0126 (Fig. 6B), during the chase period, inhibition of ERK activation by U0126 significantly accelerated the reduction of γH2AX, demonstrating that ERK activity reduces the repair of NCS-induced DSBs (Supplementary Fig. 6). Taken together, we provide compelling evidence that ERK activation negatively impacts the repair of DSBs.

3.4. Inhibition of ERK activation enhances ETOP-induced activation of DNA-PKcs

As NHEJ is one of the major process of DSB repair [2] and because ETOP-induced DSBs are repaired by NHEJ [45], the data presented above collectively support the notion that ERK activation reduces the repair of DSBs via affecting the NHEJ pathway. Activation of NHEJ starts upon the recognition of DSBs by Ku, which results in the activation of DNA-PKcs [2]. We thus reasoned that ERK activation may reduce either the recognition of DSBs by Ku or the subsequent DNA-PKcs activation. As ETOP induces comparable accumulation of Ku in the nuclei in Ctrl, shRNA, and ERK2 shRNA cells (Supplementary Fig. 7), we therefore focused on the latter possibility.

Phosphorylation of DNA-PKcs at S2056 is mediated by DNA-PKcs and is therefore widely used to detect the activation of DNA-PKcs [16,17]. While inhibition of ERK activation by U0126 does not alter the expression of DNA-PKcs and the Ku proteins (Fig. 7A, left panel), U0126 significantly enhances DNA-PKcs activation compared to DMSO treatment (Fig. 7A). In line with these observations, inhibition of ERK activation by the dominant negative MEK1K97M increased ETOP-induced DNA-PKcs activation and conversely enforced activation of ERK by expressing the constitutively active MEK1Q56P reduced this event (Fig. 7B). Furthermore, knockdown of either ERK1 or ERK2 also elevated ETOP-induced activation of DNA-PKcs (Fig. 8A). In comparison

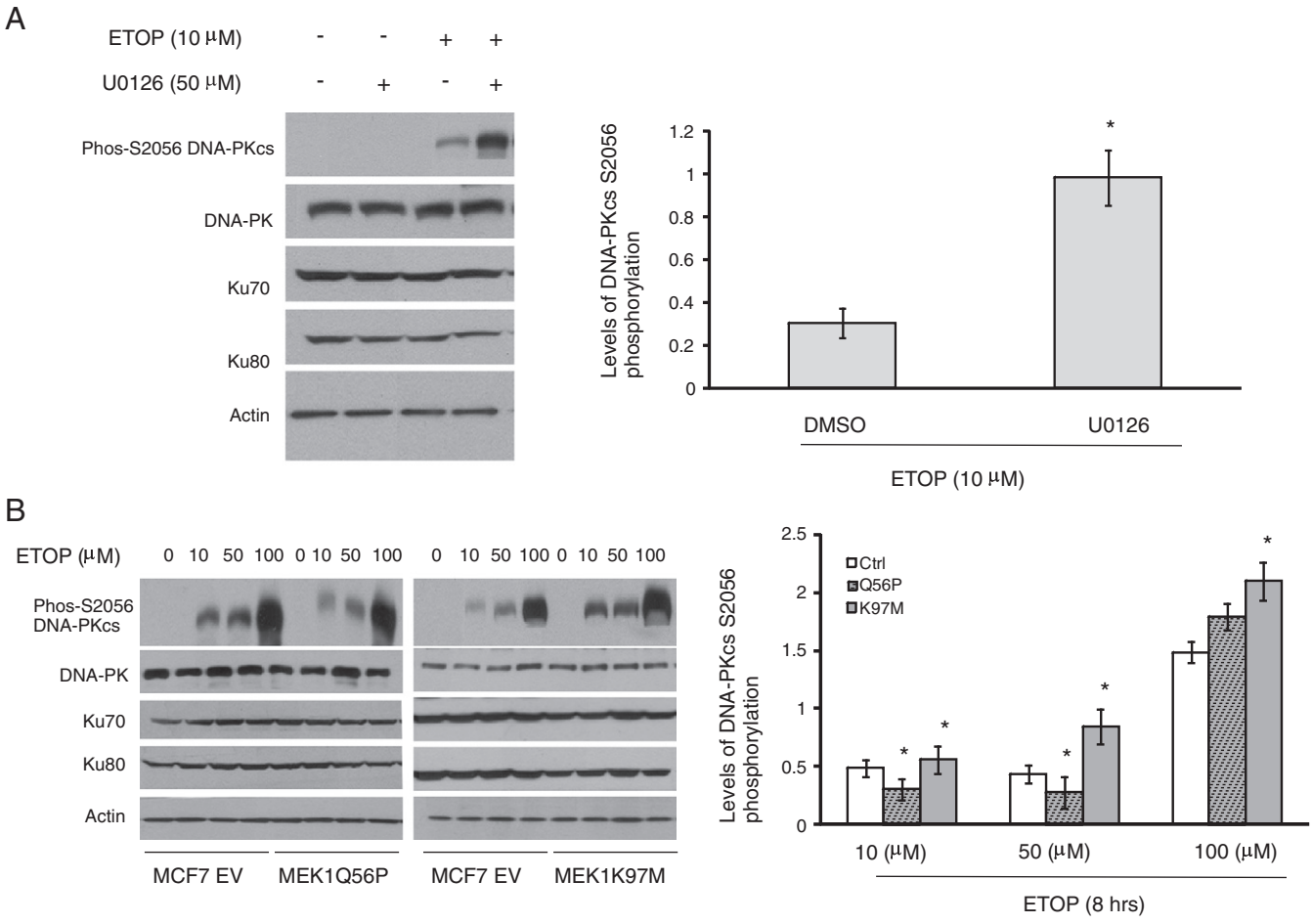

Fig. 7. Modulation of MEK-mediated ERK activation affects ETOP-induced activation of DNA-PKcs. (A) MCF7 cells were pre-treated for 30 min with DMSO (−) or U0126 (50 μM), followed by addition of ETOP and U0126 at the indicated combinations for 8 h. Phosphorylation of DNA-PKcs at S2056 (Phos-S2056 DNA-PKcs), DNA-PKcs, Ku70, Ku80, and actin were examined by western blot (left panel). Levels of Phos-S2056 DNA-PKcs were quantified against the respective DNA-PKcs. Experiments were repeated three times. Means and standard errors are presented. *: statistically significant ($p<0.05$) compared to the DMSO treatment (right panel). (B) MCF7 EV (empty vector), MEK1Q56P, and MEK1K97M cells were either mock-treated (0: DMSO) or treated with ETOP at the indicated doses for 8 h, followed by examination of Phos-S2056 DNA-PKcs, DNA-PKcs, Ku70, Ku80, and actin by western blot (left panel). Experiments were repeated three times. Phos-S2056 DNA-PKcs was quantified and presented as above. *: statistically significant ($p<0.05$) in comparison to EV cells (right panel).

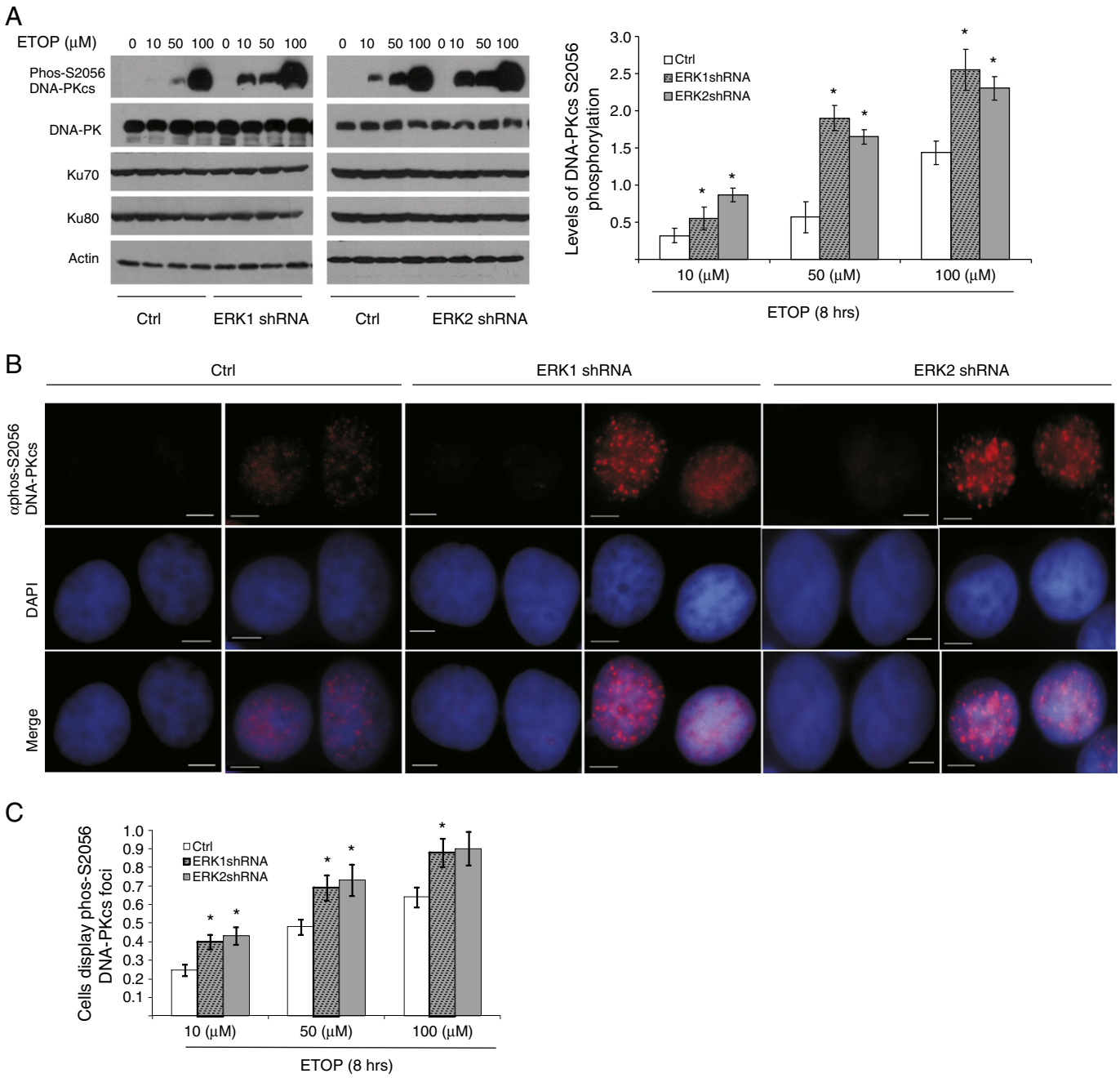

Fig. 8. Knockdown of ERK1 or ERK2 promotes ETOP-induced activation of DNA-PKcs. (A) MCF7 Ctrl, ERK1 shRNA, and ERK2 shRNA cells were either mock-treated (0: DMSO) or treated with ETOP at the indicated doses for 8 h, followed by the examination of Phos-S2056 DNA-PKcs, DNA-PKcs, Ku70, Ku80, and actin by western blot (left panel). Experiments were repeated three times. Phos-S2056 DNA-PKcs was quantified and presented as above. *: statistically significant ($p<0.05$) in comparison to Ctrl cells (right panel). (B) The indicated cell lines were treated with 10 μM ETOP for 8 h, followed by immunofluorescent staining for phos-S2056 DNA-PKcs. Typical images are shown. Scale bars represent 5 μm. (C) Cells were treated as indicated. The percentage of cells displaying phos-S2056 DNA-PKcs foci was determined by randomly counting 200 cells in several fields. Experiments were repeated three times. Means and standard errors are presented. *: statistically significant ($p<0.05$) in comparison to the respective Ctrl cell populations.

with control cells, ERK1 shRNA and ERK2 shRNA cells displayed a substantial increase in the nuclear foci of S2056 phosphorylated DNA-PKcs (Fig. 8B). Additionally, more number of ERK1 shRNA or ERK2 shRNA cells displayed the nuclear foci of S2056-phosphorylated DNA-PKcs than Ctrl cells (Fig. 8C, Supplementary Fig. 8).

4. Discussion

Accumulating evidence reveals the involvement of the MEK–ERK pathway in the activation of DNA damage checkpoints during DDR [31,26]. Adding to this knowledge, we demonstrated that the MEK–ERK pathway, surprisingly, reduces NHEJ-mediated repair of DSBs via attenuation of DNA-PKcs activation. As ETOP induced DSBs by "poisoning" topoisomerase II [37], it is possible that ERK kinase activity may rescue topoisomerase II from being poisoned by ETOP, and thereby attenuating ETOP-induced DSBs. However, our research clearly excluded this possibility. 1) Upon exposure of ETOP for 30 min, comparable amounts of DSBs were detected in cells with or without ERK kinase activation being altered (Figs. 2, 4, 5); 2) It is in the chase phase that ERK activity was found to reduce DSB repair (Figs. 4, 5); 3) ERK activity also attenuates the repair of NCS-induced DSBs (Fig. 6). Collectively, we have demonstrated that ERK activity delays NHEJ-mediated repair of DSBs. Our research is consistent with a recent report showing that inhibition of p38 MAPK stimulates the repair

of DSB via homologous recombination (HR) [31]. Therefore, it is tempting to propose that MAP kinases in general attenuate the repair of DSBs via either NHEJ (ERK MAPK, this study) or homologous recombination (p38 MAPK) [31].

ERK activation via oncogenic RAF has been reported to facilitate HR [31]. As HR occurs in late S and G2 phases and because ERK kinases are well known to promote cell cycle progression, it remains to be seen whether ERK kinases facilitate HR by directly affecting the HR machinery or by indirectly accelerating cell cycle progression. Although it has been reported that the MEK–ERK pathway contributed to EGFR-sensitized NHEJ- and HR-mediated repair of IR-induced DSBs in A549, H1299, and U87 cells [46,47], it was not clear whether this was caused by interplays between the MEK–ERK system and the rest of EGFR-activated signalling network. Additionally, as both reports relied solely on using inhibitors, the concept that the MEK–ERK pathway enhances the repair of IR-induced DSBs via NHEJ needs to be confirmed. However, it is also possible that the differences between their studies and our investigation may be attributable to different cell lines and DSB-inducing reagents being used. Nonetheless, in our research, we demonstrated that ERK reduces NHEJ via inhibition of DNA-PKcs activation via a variety of approaches, including using U0126, dominant negative MEK1K97M, constitutively active MEK1Q56P, and knockdown of either ERK1 or ERK2. Although we cannot exclude the possibility that ERK may also reduce steps downstream of DNA-PK in the NHEJ cascade, our observation that ERK kinases affect the activation of DNA-PKcs is consistent with their involvement in activation of other PIKK members, ATM [31,32] and ATR [25,33].

While individual mechanisms are certainly in place to activate ATM, ATR, and DNA-PKcs, their activation shares core features: interaction with specific binding partners and association with DNA lesions [10]. As threshold levels of ERK activity are required for the proper recruitment of ATM and ATR to DNA lesions [31–33], it is tempting to propose that ERK activity may either directly or indirectly reduce the association of DNA-PKcs with DNA-associated Ku. Alternatively, by attenuating DNA-PKcs activation, ERK activity may reduce the dissociation of DNA-PKcs from dsDNA ends. This is because autophosphorylation induces conformation changes in DNA-PKcs [17], leading to its dissociation from dsDNA ends [13,48], a critical event that is required for NHEJ [2]. Further research, however, is needed to address the underlying mechanisms responsible for ERK-mediated attenuation of DNA-PKcs activation.

Although PIKKs are critical kinases in regulating DDR and their activation coordinates the execution of DDR in terms of damage repair and activation of cell cycle checkpoints [49,50], it is, however, unclear how this coordination is achieved. It is, thus, intriguing to see that ERK kinases facilitate the activation of ATM and ATR [31–33], and at the same time attenuates the activation of another PIKK member, DNA-PKcs. As ATM and DNK-PKcs are both activated by DSBs [51,2], we may envisage a scenario in which ERK kinases differentially regulate the activation of DNA-PKcs and ATM. Activation of ATM is mediated by MRN (MRE11/RAD50/NBS1) [52–54]. The MRN complex recognizes DSBs to initiate HR that takes place in S and G2 phases, while NHEJ is not generally restricted to specific phases of the cell cycle [2]. ERK kinases promote cell cycle progression and facilitate DSB-induced G2/M arrest [32]. As DSBs are repaired mainly by either HR or NHEJ [2], it is thus plausible that ERK kinases, upon activation by DNA damage, slow down NHEJ-mediated repair of DSBs via reducing DNA-PKcs activation in order to leave DSBs to be repaired by HR. As HR is an error-free process in comparison with the error-prone process of NHEJ-mediated DSB repair [55,2], this setting would therefore enhance the fidelity of DSB repair. Interestingly, this hypothesis is consistent with the observations that ERK kinases facilitate HR-mediated repair of DSBs [31].

Regardless of what might be the biological impact of the observed differential regulation of PIKK activation by the ERK kinases during DDR, it seems a common theme that the MEK–ERK pathway regulates the proper activation of PIKK members, including ATM, ATR, and DNA-PKcs.

Acknowledgments

The authors would like to thank Dr. Chatterjee for providing ERK shRNA constructs. We also like to acknowledge the financial support from St. Joseph's HealthCare at Hamilton, Ontario, Canada to the Hamilton Centre for Kidney Research (HCKR).

Funding for open access charge: A CIHR grant (MOP – 84381) to D. Tang and the Hamilton Centre for Kidney Research, St. Joseph's HealthCare at Hamilton, Ontario, Canada.

Appendix A. Supplementary data

Supplementary data to this article can be found online at http://dx.doi.org/10.1016/j.bbamcr.2012.10.016.

References

[1] S.J. Collis, T.L. DeWeese, P.A. Jeggo, A.R. Parker, The life and death of DNA-PK, Oncogene 24 (2005) 949–961.
[2] B.L. Mahaney, K. Meek, S.P. Lees-Miller, Repair of ionizing radiation-induced DNA double-strand breaks by non-homologous end-joining, Biochem. J. 417 (2009) 639–650.
[3] D. Moshous, I. Callebaut, R. de Chasseval, B. Corneo, M. Cavazzana-Calvo, F. Le Deist, I. Tezcan, O. Sanal, Y. Bertrand, N. Philippe, A. Fischer, J.P. de Villartay, Artemis, a novel DNA double-strand break repair/V(D)J recombination protein, is mutated in human severe combined immune deficiency, Cell 105 (2001) 177–186.
[4] E.R. Phillips, P.J. McKinnon, DNA double-strand break repair and development, Oncogene 26 (2007) 7799–7808.
[5] K. Meek, S. Gupta, D.A. Ramsden, S.P. Lees-Miller, The DNA-dependent protein kinase: the director at the end, Immunol. Rev. 200 (2004) 132–141.
[6] K. Meek, V. Dang, S.P. Lees-Miller, DNA-PK: the means to justify the ends? Adv. Immunol. 99 (2008) 33–58.
[7] D.C. van Gent, M. van der Burg, Non-homologous end-joining, a sticky affair, Oncogene 26 (2007) 7731–7740.
[8] Q. Ding, Y.V. Reddy, W. Wang, T. Woods, P. Douglas, D.A. Ramsden, S.P. Lees-Miller, K. Meek, Autophosphorylation of the catalytic subunit of the DNA-dependent protein kinase is required for efficient end processing during DNA double-strand break repair, Mol. Cell. Biol. 23 (2003) 5836–5848.
[9] K.A. Cimprich, D. Cortez, ATR: an essential regulator of genome integrity, Nat. Rev. Mol. Cell Biol. 9 (2008) 616–627.
[10] A.E. Burrows, S.J. Elledge, How ATR turns on: TopBP1 goes on ATRIP with ATR, Genes Dev. 22 (2008) 1416–1421.
[11] T.M. Gottlieb, S.P. Jackson, The DNA-dependent protein kinase: requirement for DNA ends and association with Ku antigen, Cell 72 (1993) 131–142.
[12] N. Uematsu, E. Weterings, K. Yano, K. Morotomi-Yano, B. Jakob, G. Taucher-Scholz, P.O. Mari, D.C. van Gent, B.P. Chen, D.J. Chen, Autophosphorylation of DNA-PKCS regulates its dynamics at DNA double-strand breaks, J. Cell Biol. 177 (2007) 219–229.
[13] D.W. Chan, S.P. Lees-Miller, The DNA-dependent protein kinase is inactivated by autophosphorylation of the catalytic subunit, J. Biol. Chem. 271 (1996) 8936–8941.
[14] P. Douglas, G.P. Sapkota, N. Morrice, Y. Yu, A.A. Goodarzi, D. Merkle, K. Meek, D.R. Alessi, S.P. Lees-Miller, Identification of in vitro and in vivo phosphorylation sites in the catalytic subunit of the DNA-dependent protein kinase, Biochem. J. 368 (2002) 243–251.
[15] X. Cui, Y. Yu, S. Gupta, Y.M. Cho, S.P. Lees-Miller, K. Meek, Autophosphorylation of DNA-dependent protein kinase regulates DNA end processing and may also alter double-strand break repair pathway choice, Mol. Cell. Biol. 25 (2005) 10842–10852.
[16] P. Douglas, X. Cui, W.D. Block, Y. Yu, S. Gupta, Q. Ding, R. Ye, N. Morrice, S.P. Lees-Miller, K. Meek, The DNA-dependent protein kinase catalytic subunit is phosphorylated in vivo on threonine 3950, a highly conserved amino acid in the protein kinase domain, Mol. Cell. Biol. 27 (2007) 1581–1591.
[17] E.P. Morris, A. Rivera-Calzada, P.C. da Fonseca, O. Llorca, L.H. Pearl, L. Spagnolo, Evidence for a remodelling of DNA-PK upon autophosphorylation from electron microscopy studies, Nucleic Acids Res. 39 (2011) 5757–5767.
[18] W. Kolch, Meaningful relationships: the regulation of the Ras/Raf/MEK/ERK pathway by protein interactions, Biochem. J. 351 (2000) 289–305.
[19] J. Krepinsky, D. Wu, A. Ingram, J. Scholey, D. Tang, Developments in mitogen-induced extracellular kinase 1 inhibitors and their use in the treatment of disease, Expert Opin. Ther. Pat. 12 (2002) 1795–1811.
[20] D.L. Persons, E.M. Yazlovitskaya, J.C. Pelling, Effect of extracellular signal-regulated kinase on p53 accumulation in response to cisplatin, J. Biol. Chem. 275 (2000) 35778–35785.

[21] S.W. Lee, L. Fang, M. Igarashi, T. Ouchi, K.P. Lu, S.A. Aaronson, Sustained activation of Ras/Raf/mitogen-activated protein kinase cascade by the tumor suppressor p53, Proc. Natl. Acad. Sci. U. S. A. 97 (2000) 8302–8305.
[22] X. Wang, J.L. Martindale, N.J. Holbrook, Requirement for ERK activation in cisplatin-induced apoptosis, J. Biol. Chem. 275 (2000) 39435–39443.
[23] D. Tang, D. Wu, A. Hirao, J.M. Lahti, L. Liu, B. Mazza, V.J. Kidd, T.W. Mak, A.J. Ingram, ERK activation mediates cell cycle arrest and apoptosis after DNA damage independently of p53, J. Biol. Chem. 277 (2002) 12710–12717.
[24] J.W. Pippin, R. Durvasula, A. Petermann, K. Hiromura, W.G. Couser, S.J. Shankland, DNA damage is a novel response to sublytic complement C5b-9-induced injury in podocytes, J. Clin. Invest. 111 (2003) 877–885.
[25] D. Wu, B. Chen, K. Parihar, L. He, C. Fan, J. Zhang, L. Liu, A. Gillis, A. Bruce, A. Kapoor, D. Tang, ERK activity facilitates activation of the S-phase DNA damage checkpoint by modulating ATR function, Oncogene 25 (2006) 1153–1164.
[26] Y. Yan, C.P. Black, K.H. Cowan, Irradiation-induced G2/M checkpoint response requires ERK1/2 activation, Oncogene 26 (2007) 4689–4698.
[27] J.H. Lee, K.T. Kim, Regulation of cyclin-dependent kinase 5 and p53 by ERK1/2 pathway in the DNA damage-induced neuronal death, J. Cell. Physiol. 210 (2007) 784–797.
[28] V. Mogila, F. Xia, W.X. Li, An intrinsic cell cycle checkpoint pathway mediated by MEK and ERK in *Drosophila*, Dev. Cell 11 (2006) 575–582.
[29] Y. Dai, S. Chen, X.Y. Pei, J.A. Almenara, L.B. Kramer, C.A. Venditti, P. Dent, S. Grant, Interruption of the Ras/MEK/ERK signaling cascade enhances Chk1 inhibitor-induced DNA damage in vitro and in vivo in human multiple myeloma cells, Blood 112 (2008) 2439–2449.
[30] C. Nishioka, T. Ikezoe, J. Yang, A. Yokoyama, Inhibition of MEK signaling enhances the ability of cytarabine to induce growth arrest and apoptosis of acute myelogenous leukemia cells, Apoptosis 14 (2009) 1108–1120.
[31] S.E. Golding, E. Rosenberg, S. Neill, P. Dent, L.F. Povirk, K. Valerie, Extracellular signal-related kinase positively regulates ataxia telangiectasia mutated, homologous recombination repair, and the DNA damage response, Cancer Res. 67 (2007) 1046–1053.
[32] F. Wei, Y. Xie, L. Tao, D. Tang, Both ERK1 and ERK2 kinases promote G2/M arrest in etoposide-treated MCF7 cells by facilitating ATM activation, Cell. Signal. 22 (2010) 1783–1789.
[33] F. Wei, Y. Xie, H. Lizh, L. Tao, D. Tang, ERK1 and ERK2 kinases activate hydroxyurea-induced S-phase checkpoint in MCF7 cells by mediating ATR activation, Cell. Signal. 23 (2011) 259–268.
[34] M. Chatterjee, T. Stuhmer, P. Herrmann, K. Bommert, B. Dorken, R.C. Bargou, Combined disruption of both the MEK/ERK and the IL-6R/STAT3 pathways is required to induce apoptosis of multiple myeloma cells in the presence of bone marrow stromal cells, Blood 104 (2004) 3712–3721.
[35] N.P. Singh, M.T. McCoy, R.R. Tice, E.L. Schneider, A simple technique for quantitation of low levels of DNA damage in individual cells, Exp. Cell Res. 175 (1988) 184–191.
[36] H.C. Wang, W.C. Chou, S.Y. Shieh, C.Y. Shen, Ataxia telangiectasia mutated and checkpoint kinase 2 regulate BRCA1 to promote the fidelity of DNA end-joining, Cancer Res. 66 (2006) 1391–1400.
[37] P.S. Kingma, N. Osheroff, The response of eukaryotic topoisomerases to DNA damage, Biochim. Biophys. Acta 1400 (1998) 223–232.
[38] A.R. Collins, A.A. Oscoz, G. Brunborg, I. Gaivão, L. Giovannelli, M. Kruszewski, C.C. Smith, R. Stetina, The comet assay: topical issues, Mutagenesis 23 (2008) 143–151.
[39] D.G. McArt, G. McKerr, C.V. Howard, K. Saetzler, G.R. Wasson, Modelling the comet assay, Biochem. Soc. Trans. 37 (2009) 914–917.
[40] J. Dierov, R. Dierova, M. Carroll, BCR/ABL translocates to the nucleus and disrupts an ATR-dependent intra-S phase checkpoint, Cancer Cell 5 (2004) 275–285.
[41] J.G. Turner, D.C. Marchion, J.L. Dawson, M.F. Emmons, L.A. Hazlehurst, P. Washausen, D.M. Sullivan, Human multiple myeloma cells are sensitized to topoisomerase II inhibitors by CRM1 inhibition, Cancer Res. 69 (2009) 6899-6805.
[42] A.C. Teixeira, R.A. Dos Santos, A. Poersch, H.H. Carrara, J.M. de Andrade, C.S. Takahashi, DNA repair in Etoposide-induced DNA damage in lymphocytes of breast cancer patients and healthy women, Int. J. Clin. Exp. Med. 2 (2009) 280–288.
[43] A. Shahi, J.H. Lee, Y. Kang, S.H. Lee, J.W. Hyun, I.Y. Chang, J.Y. Jun, H.J. You, Mismatch-repair protein MSH6 is associated with Ku70 and regulates DNA double-strand break repair, Nucleic Acids Res. 39 (2011) 2130–2143.
[44] G.M. Kavanaugh, T.M. Wise-Draper, R.J. Morreale, M.A. Morrison, B. Gole, S. Schwemberger, E.D. Tichy, L. Lu, G.F. Babcock, J.M. Wells, R. Drissi, J.J. Bissler, P.J. Stambrook, P.R. Andreassen, L. Wiesmüller, S.I. Wells, The human DEK oncogene regulates DNA damage response signaling and repair, Nucleic Acids Res. 39 (2011) 7465–7476.
[45] V. Quennet, A. Beucher, O. Barton, S. Takeda, M. Löbrich, CtIP and MRN promote non-homologous end-joining of etoposide-induced DNA double-strand breaks in G1, Nucleic Acids Res. 39 (2011) 2144–2152.
[46] S.E. Golding, R.N. Morgan, B.R. Adams, A.J. Hawkins, L.F. Povirk, K. Valerie, Pro-survival AKT and ERK signaling from EGFR and mutant EGFRvIII enhances DNA double-strand break repair in human glioma cells, Cancer Biol. Ther. 8 (2009) 730–738.
[47] M. Kriegs, U. Kasten-Pisula, T. Rieckmann, K. Holst, J. Saker, J. Dahm-Daphi, E. Dikomey, DNA repair, DNA Repair 9 (2010) 889–897.
[48] D. Merkle, P. Douglas, G.B. Moorhead, Z. Leonenko, Y. Yu, D. Cramb, D.P. Bazett-Jones, S.P. Lees-Miller, The DNA-dependent protein kinase interacts with DNA to form a protein-DNA complex that is disrupted by phosphorylation, Biochemistry 41 (2002) 12706–12714.
[49] S. Bhattacharya, R.M. Ray, L.R. Johnson, Role of polyamines in p53-dependent apoptosis of intestinal epithelial cells, Cell. Signal. 21 (2009) 509–522.
[50] M.T. Mok, B.R. Henderson, A comparison of BRCA1 nuclear localization with 14 DNA damage response proteins and domains: identification of specific differences between BRCA1 and 53BP1 at DNA damage-induced foci, Cell. Signal. 22 (2010) 47–56.
[51] B.B. Zhou, S.J. Elledge, The DNA damage response: putting checkpoints in perspective, Nature 408 (2000) 433–439.
[52] J.H. Lee, T.T. Paull, ATM activation by DNA double-strand breaks through the Mre11-Rad50-Nbs1 complex, Science 308 (2005) 551–554.
[53] S. Difilippantonio, A. Celeste, O. Fernandez-Capetillo, H.T. Chen, B. Reina San Martin, F. Van Laethem, Y.P. Yang, G.V. Petukhova, M. Eckhaus, L. Feigenbaum, K. Manova, M. Kruhlak, R.D. Camerini-Otero, S. Sharan, M. Nussenzweig, A. Nussenzweig, Role of Nbs1 in the activation of the Atm kinase revealed in humanized mouse models, Nat. Cell Biol. 7 (2005) 675–685.
[54] J. Falck, J. Coates, S.P. Jackson, Conserved modes of recruitment of ATM, ATR and DNA-PKcs to sites of DNA damage, Nature 434 (2005) 605–611.
[55] P.A. Jeggo, M. Löbrich, DNA double-strand breaks: their cellular and clinical impact? Oncogene 26 (2007) 7717–7719.